

From *para*-Dimethoxybenzene Toward Crownbenzenophanes, 2^[1]

Synthesis, X-ray Structure and Fluorescence Emission Properties of 1,3,10,13,16,19,22-Heptaoxa(3,13)[28]paracyclophane and Its Complex with Sodium Cation

Pierre Marsau^{*a}, Harimbola Andrianatoandro^a, Thomas Willms^{†*†}, Jean-Pierre Desvergne^{*b}, Henri Bouas-Laurent^b, Henning Hopf^{*c}, and Ralf Utermöhlen^{†*†}

Laboratoire de Cristallographie et Physique Cristalline^a,
Université Bordeaux 1, F-33405 Talence Cedex, France

Photophysique et Photochimie Moléculaire, URA 348^b,
Université Bordeaux 1, F-33405 Talence Cedex, France

Institut für Organische Chemie, Technische Universität Braunschweig^c,
Hagenring 30, W-3300 Braunschweig, F. R. G.

Received November 9, 1992

Key Words: Supramolecular chemistry / Crown ethers / Phanes / Fluid solutions and single crystals, spectroscopic properties of

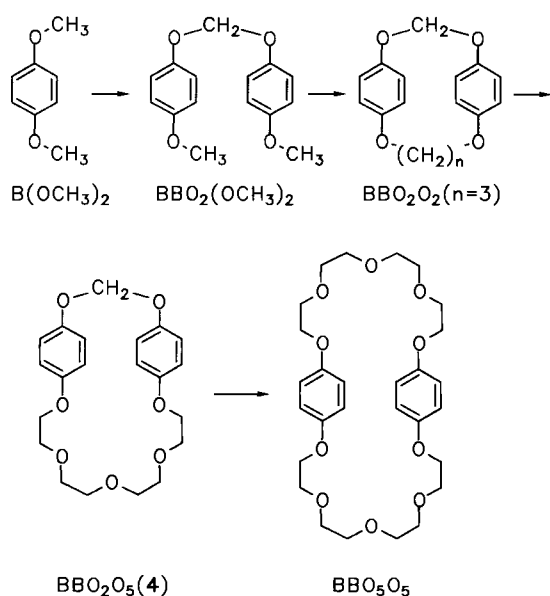
The synthesis and X-ray molecular structure of the title compound, an heptaoxa[3,13]paracyclophane, as well as that of its 1:1 sodium complex are described; a study of the absorption

and fluorescence spectra indicates that this crown-cyclophane behaves as a hybrid between strained classical cyclophanes and large macrocycles.

Since the discovery of cyclophanes by Cram^[2a], the field has experienced a continuous expansion^[2b-c], especially in the size and structural complexity of the rings, the large

cyclophanes being now designed for the complexation of metal ions and neutral or ionic molecules. This is particularly well-illustrated by the crown-ether BBO₅O₅ (Scheme 1) used by Stoddard^[3] to generate new catenanes and rotaxanes of great interest. But in these macrocyclic compounds, the intramolecular interaction between the two benzene rings, which is characteristic of small-ring cyclophanes, seems to vanish.

Scheme 1. Structural analogy between crownbenzenophane BBO₅O₅ and *para*-dimethoxybenzene; illustration of the stepwise construction of large parabenzenophanes through medium-sized rings keeping the properties of the classical phanes (budding crownbenzenophanes)



From the observation that BBO₅O₅ incorporates two *p*-dimethoxybenzene units which could be assembled in molecules of progressive complexity such as BBO₂O₂ and BBO₂O₅ (Scheme 1), it was expected to trace the evolution of the properties from a simple *para*-disubstituted benzene derivative to an elaborate crown ether; in particular, it was interesting to investigate the “point of no return” between the classical phanes and the complexing crown ethers.

In a first paper^[1], we have described the preparation and the structural and spectral properties of the three first members of the series represented in Scheme 1. The new [3.5]tetraoxaphane [BBO₂O₂ (*n* = 3)] was found to behave as a classical cyclophane in exhibiting strong interactions between the two aromatic rings, and special properties conferred by the donating properties of the substituent were observed.

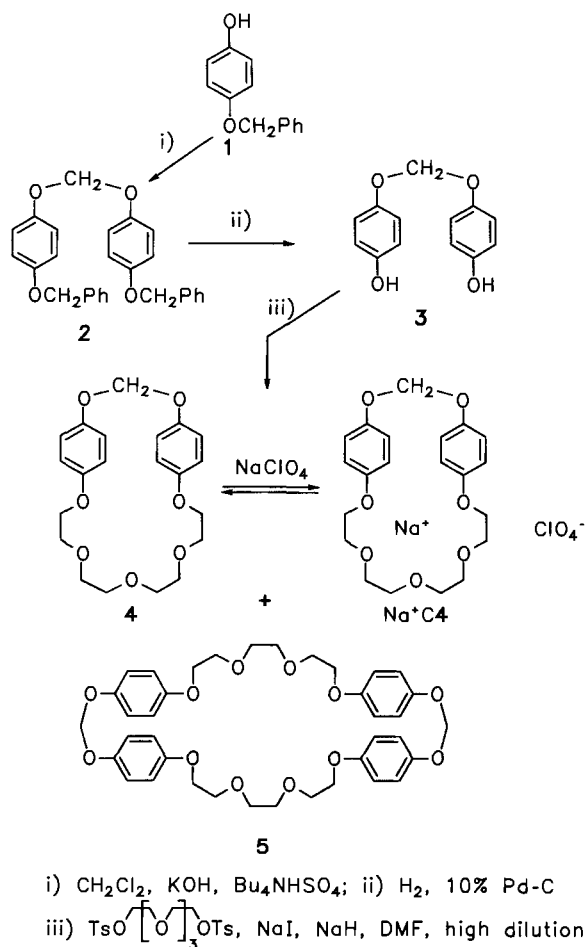
In this article, we describe the synthesis of the fourth member [BBO₂O₅ (**4**)], the X-ray molecular structure of the free ligand as well as that of the sodium complex and report a study of the electronic spectra. From the preceding work, it was anticipated that **4** would behave as a hybrid between classical cyclophanes and crown ethers, and we show that it is indeed the case.

^[*†] Erasmus student (1990–1991). — ^[†*†] Procope awardee (1989–1991).

Synthesis

The preparation of compound **4** is outlined in Scheme 2. The starting material, *p*-benzyloxyphenol (**1**) is commercial; it is smoothly transformed into **2** by using the Dehmlo reaction^[1]; deprotection of **2** by hydrogenolysis generates the diphenol **3** which is the precursor of **4**. These reactions have been described in the preceding paper^[1]. The one-pot reaction leading to **4** was conducted under high dilution^[4] in dimethylformamide at 100 °C under nitrogen; the tetraethyleneglycol ditosylate was mixed with sodium iodide to accelerate the S_N2 reactions. In addition to **4**, a second product was isolated which was identified as its dimer **5**, and both were fully characterized by the spectroscopic data in agreement with the proposed structures. The yields are poor (2–3%), but they were not optimized.

Scheme 2. Synthesis of compounds **4** and **5**



X-ray Crystal Structure

The molecular structure of **4** could be definitely established by X-ray crystallography from single crystals of the free ligand which were obtained by slow evaporation of solutions of **4** in a 1:1 (v/v) mixture of CH_3OH and toluene. Moreover, by adding a 2–3 molar excess of NaClO_4 to such a solution, single crystals of the 1:1 complex $\text{Na}^+ \subset \mathbf{4}$ were grown. Both structures were resolved. The structures

of **4** and $\text{Na}^+ \subset \mathbf{4}$ are represented in Figure 1 and Figure 2. However, no single crystals could be obtained for the amorphous compound **5**. It is noteworthy that the crystal of the complex incorporates one molecule of water per unit cell with the result that the shortest distances $\text{Na} \cdots \text{O}$ (2.31–2.59 Å) are found between 4 oxygen atoms of the crown ether, the counter ion and one molecule of H_2O .

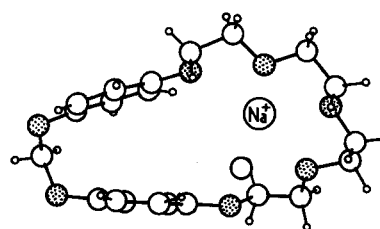
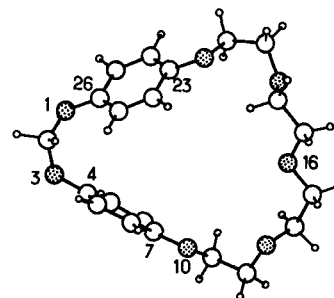


Figure 1. Projection of compound **4** along one of the benzene ring planes (top); projection of complex $\text{Na}^+ \subset \mathbf{4}$ along one of the benzene ring planes (bottom)

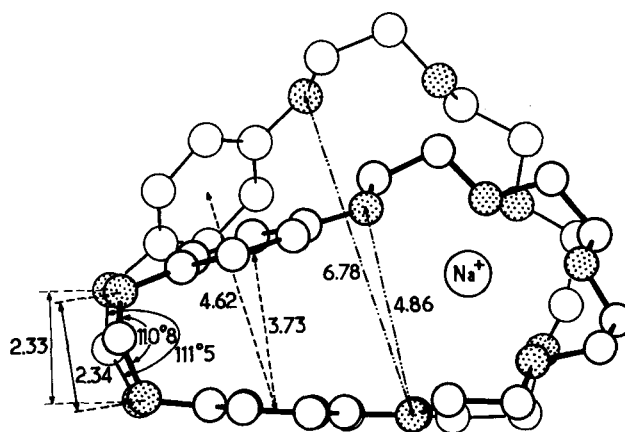


Figure 2. Superimposition of **4** and $\text{Na}^+ \subset \mathbf{4}$ showing the conformational modifications induced by complexation of a sodium cation solvated by 4 oxygen atoms of the crown ether, the counterion and one molecule of H_2O

In **4**, the angle between the rings is ca. 62°, and the distance between the middle of the benzene nuclei is 460 pm. The complexation entails important geometric changes; the angle between the rings is reduced to 20° and the inter-ring distance becomes 370 pm; the latter is an average as the distance between the bridgehead atoms is 307 pm whereas it is 435 pm between the more remote aromatic carbon atoms.

Spectroscopic Properties

a) Electronic Absorption

The absorption spectra of **4** and **5** are weakly sensitive to solvent (in Et₂O, CH₂Cl₂, MeOH, CH₃CN); they are represented in CH₃OH (Figures 3 and 4) because of the ability of this solvent to dissolve sodium salts in high concentrations. The comparison of the UV spectrum of **4** with that of the first members of the family derived from *p*-dimethoxybenzene^[1] (Figure 3) clearly reveals that the "cyclophane character" i.e. the hypsochromic and hypochromic effects are still present but attenuated as compared with those of BBO₂O₂ (*n* = 3), the [3.5]cyclophane. Conversely, as depicted in the inset, the dimer (**5**) in which the two benzene rings experience much less conformational constraints consistently exhibits an absorption similar to that of *p*-dimethoxybenzene.

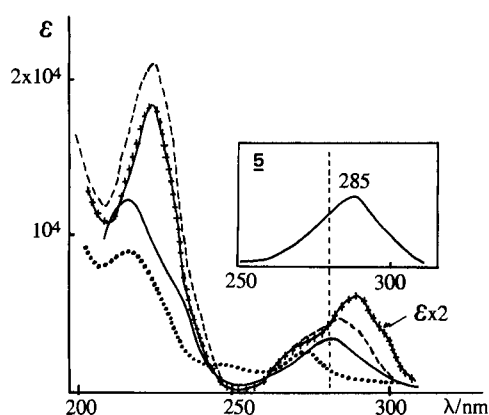


Figure 3. Electronic absorption spectra in CH₃OH (20 °C) of *p*-dimethoxybenzene [B(OCH₃)₂] (++++); bichromophore BBO₂(OCH₃)₂ (-----); cyclophane BBO₂O₂ (.....); and **4** (—); in the inset the lower energy band of **5** is represented in the same solvent (the intensity is in arbitrary units)

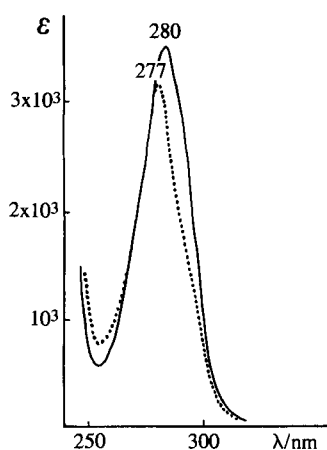


Figure 4. Electronic absorption spectra in CH₃OH (25 °C) of **4** (conc. ca. 2×10^{-4} M) (—) and **4** + NaClO₄ in large excess (conc. ca. 1 M) (.....)

The addition of NaClO₄ (the best host-guest fit for a crown ether made of five oxygen atoms is known to be with Na⁺^[4c]) up to 500 molar equivalents does not alter the UV

spectrum of **4**. A large excess (≥ 5000 molar equiv.) is necessary to form a complex and displace the UV spectrum (slight hypso- and hypochromic effect) (Figure 4). This points to a poor complexation ability of **4** in methanol.

b) Fluorescence Emission

The fluorescence spectra of **4** and **5** in methanol solution are given in Figure 5; they differ markedly from each other: **5** shows essentially the characteristics of the *p*-dimethoxybenzene monomer with an emission peak at $\lambda = 315$ nm accompanied by some excimer^[5] emission (λ_{max} 370 nm) whereas **4** has an excimer band more intense than the monomer band; this is consistent with an average closer distance between the two benzene rings in **4** which results in a better ability to form an excimer. Moreover, the fluorescence quantum yields determined in MeOH for **4** ($\Phi_F = 0.02$) and **5** ($\Phi_F = 0.09$) are in keeping with the above observation; the quantum yield of **4** is the same as that of BBO₂O₂ (*n* = 3)^[1], but the quantum yield of **5** is similar to that of the bichromophore BBO₂(OCH₃)₂^[1]. Indeed, as indicated in the preceding paper^[1], the stronger the inter-ring interaction, the lower the quantum yield.

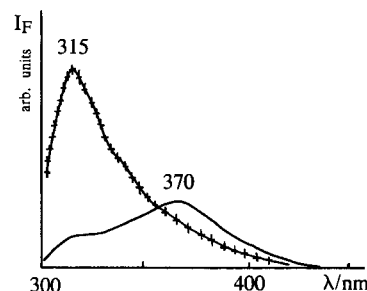


Figure 5. Corrected fluorescence spectra ($\lambda_{\text{exc.}} = 280$ nm) in CH₃OH of **4** (conc. ca. 10^{-5} M) (—) and **5** (x x x) at room temperature

That the excimer formation is dependent on the chain conformation is evident from the influence of the complexation with NaClO₄ (Figure 6); the progressive addition of salt solution aliquots decreases the monomer emission to increase the excimer emission intensity; the curves have a common crossing (isoluminescent)^[6] point at $\lambda = 324$ nm. Whereas the sodium cations strengthen the excimer formation in acting on the balance between the number of excimer- versus monomer-emitting centers, they change the excimer geometry in shifting the maximum wavelength towards higher energies [from 370 nm (27027 cm^{-1}) to 362 nm (27624 cm^{-1}); $\Delta\tilde{\nu} \approx 600 \text{ cm}^{-1}$]. As it can be observed in the X-ray structures (cf. Figure 2), the sodium cation is grasped in the crown ether like a marble with tweezers; the benzene rings are maintained in a more rigid arrangement, and in the excited state they presumably have less freedom to reach the adequate excimer^[7] geometry (maximum overlap)^[5] than in the free ligand.

The single-crystal fluorescence (Figure 7) reinforces the preceding observations. The free ligand **4** exhibits essentially a monomer-like emission (with some bathochromic shift,

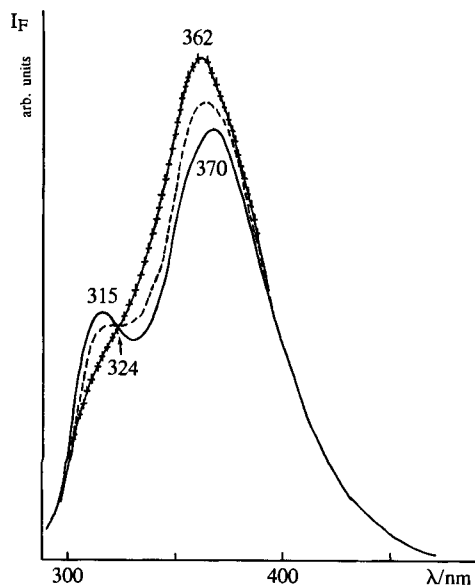


Figure 6. Corrected fluorescence spectra ($\lambda_{\text{exc}} = 280 \text{ nm}$) in CH_3OH of **4** (conc. ca. 10^{-5} M) (—), **4** + NaClO_4 in large excess (ca. 0.5 M) ($\times \times \times$) and **4** + NaClO_4 at intermediate conc. (-----); note the presence of an isolampsic^[6] point at $\lambda = 324 \text{ nm}$

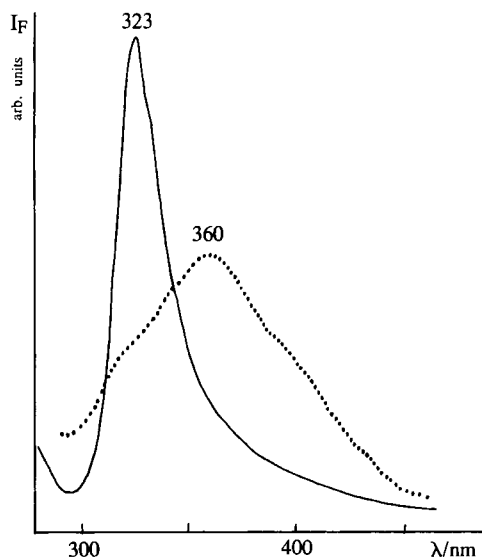


Figure 7. Single-crystal fluorescence of **4** (—) and $\text{Na}^+ \cdot \text{4}$ (.....) ($\lambda_{\text{exc}} = 280 \text{ nm}$)

probably because there is some interaction between the rings in the ground state) with little excimer (if any) formation because of the very high viscosity of the crystal. The fluorescence spectrum of the sodium complex displays a peak at $\lambda = 360 \text{ nm}$ but, in contrast with the solution, it shows some fine structure, reflecting the existence of presumably several emitting species.

Conclusion

This study is the second stage in the process of “budding benzenophanes” i.e. the stepwise construction of macrocyclic tetraoxaparacyclophanes from *p*-dialkoxybenzene units.

The data from the X-ray structure analysis of both compounds **4** and its 1:1 complex with sodium cations as well as the absorption and fluorescence spectra results clearly show that compound **4** behaves as a “hybrid cyclophane” in exhibiting properties intermediate between those of the strained classical cyclophanes and large macrocycles (such as **5**).

The next step will be the study of BBO_5O_5 , an interesting representative of this new cyclophane series as it is anticipated to generate a double salt with sodium cations, in analogy with related results^[8]. Work along these lines is in progress.

We are grateful to the *Deutscher Akademischer Austausch-Dienst* (DAAD) and the *Ministère des Affaires Étrangères* (Association Nationale de la Recherche Technique (ANRT) (France) for a “PRO-COPE” grant. One of us (H.B.-L.) is much indebted to the *Alexander-von-Humboldt Foundation* for financial assistance. We extend our thanks to Dr. *Frédéric Fages* and Miss *Christina Antonius* for assistance and to the *Fonds der Chemischen Industrie* for financial support.

Experimental

General: IR: Perkin-Elmer 1420. — UV/Vis: Varian 219 and Beckman UV 5230. — NMR: Varian EM-360, Bruker AM 400 [CDCl_3 as solvent; int. TMS as standard for ^1H NMR ($\delta = 0$) and CDCl_3 ($\delta = 77.05$) for ^{13}C NMR, respectively]; the degree of substitution of the C atoms was determined by the DEPT-135 method. — MS: Finnigan 8430 (70 eV). — Melting points (uncorrected): Büchi 510 melting point Kofler hot-stage. — Fluorescence spectra (corrected for absorption and emission): Hitachi Perkin-Elmer MPF 44 or SPEX spectrofluorimeter; fluorescence quantum yields were measured by using fluorene as external reference ($\Phi_{\text{F}} = 0.54$ in ethanol^[9] and 0.80 in cyclohexane^[10]); all fluorescence measurements were performed on samples carefully purified by HPLC [Milton-Roy HPLC-system, dichloromethane/heptane (1:1, v/v), 25 cm aminosilane column]; the various samples were degassed by the freeze-and-thaw technique until the vacuum (10^{-5} Torr) remained constant. — Analytical TLC: Sheets Polygram Sil G/UV 254 (Macherey-Nagel and Co., Düren). — Preparative column chromatography: Kieselgel 60, 70–230 mesh (Merck). — Dichloromethane, methylcyclohexane and acetonitrile were commercial high-purity solvents (Spectrosol quality); methanol was carefully distilled with a 1-m fractionating column before use.

1,3,10,13,16,19,22-Hepta-oxa(3,13)[28]paracyclophane (4) and 1,3,10,13,16,19,22,29,31,38,41,44,47,50,51-Tetradeca-oxa-(3,13,3,13)[56]paracyclophane (5): A solution of 6.00 g (25.8 mmol) of diphenol **3**^[11] and 12.2 g (25.8 mmol) of tetraethyleneglycol ditosylate in 300 ml of absolute DMF is added dropwise within 48 h (high dilution conditions) to a vigorously stirred suspension of 8.00 g (0.33 mol) of NaH and 10.0 g (66.7 mmol) of dry NaI in 1200 ml of absolute DMF maintained at 100°C under N_2 . The flask is covered with aluminium foil to prevent photochemical reactions. The mixture is then stirred for 8 h at 100°C . The DMF is distilled off under vacuum below 100°C to leave a brown oil which is dissolved in CHCl_3 ; the solution is washed twice with a solution of ammonium chloride and dried with sodium sulfate. After evaporation, the brown residue is chromatographed on SiO_2 [40-cm column; ethyl acetate/n-hexane (1:1)]; compound **4** is eluted first and forms colorless crystals, m.p. 105°C [220 mg (2.2%)]; further elution with acetone leads to the separation of compound **5** as an amorphous colorless powder, m.p. 119°C [310 mg (3.0%)].

4: IR (KBr): $\tilde{\nu} = 2920 \text{ cm}^{-1}$ (s), 2870 (s), 1510 (vs, br.), 1470 (m), 1450 (m), 1350 (m), 1300 (s), 1240 (vs, br.), 1185 (vs), 1000 (vs, br.), 820 (double, s), 725 (m). — ^1H NMR (400 MHz) ($[\text{D}_6]$ acetone): $\delta = 6.76$ (AA'BB', half spectrum, 4H, arom. H), 6.72 (AA'BB', half spectrum, 4H, arom. H), 5.70 (s, 2H), 4.07 (m, 4H), 3.68 (m, 4H), 3.51 (m, 8H). — ^{13}C NMR (100.0 MHz) (CDCl_3): $\delta = 153.7$ (s, C-4, -26), 150.6 (s, C-7, -23), 118.7 (d, C-5, -9, -25, -27), 115.6 (d, C-6, -8, -24, -26), 93.7 (t, C-2), 70.07 (t), 69.97 (t), 68.04 (t). — UV (methanol): λ_{max} (lg ϵ) = 220 nm (4.080), 260 (2.900), 270 (3.300), 280 (3.560), 300 (2.780). — MS (EI): m/z (%): 390 (100) [M^+], 232 (1), 149 (22), 137 (14), 136 (14), 123 (19), 110 (13), 76 (22).

$\text{C}_{21}\text{H}_{26}\text{O}_7$ (390.48) Calcd. C 64.60 H 6.71
Found C 65.06 H 6.96

5: IR (KBr): $\tilde{\nu} = 2920 \text{ cm}^{-1}$ (m), 2840 (m), 1510 (vs), 1455 (m), 1300 (m), 1210 (vs, br.), 1150 (vs), 1040 (vs), 820 (s), 740 (m). — ^1H NMR (250 MHz), CDCl_3 : $\delta = 6.95$ (AA'BB', half spectrum, 8H, arom. H), 6.78 (AA'BB', half spectrum, 8H, arom. H), 5.50 (s, 4H), 4.02 (m, 8H), 3.69 (m, 16H). — ^{13}C NMR (100 MHz) (CDCl_3): $\delta = 152.7$ (s, C-4, -26, -32, -54), 150.3 (s, C-7, -23, -35, -51), 118.2 (d, C-5, -9, -25, -27, -33, -37, -53, -55), 115.6 (d, C-6, -8, -24, -26, -34, -36, -52, -56), 93.8 (t, C-2), 71.07 (t), 69.36 (t), 68.9 (t), 68 (t). — UV (methanol): λ_{max} (lg ϵ) = 220 nm, 285 (owing to the extremely poor solubility, the ϵ data are not given). — MS (EI); m/z (%): 780 (30) [M^+], 402 (18), 390 (100), 199 (1), 149 (22), 137 (14), 136 (14), 123 (19), 110 (13), 76 (22).

X-ray Structure Determination^[11]. — *General*: The single-crystal X-ray data sets were collected on a C.A.D.4 diffractometer (ENRAF NONIUS) at room temperature by using graphite-monochromated Cu-K_α radiation. Three reference reflections were measured every 100 reflections, and no significant changes in intensities were noted. Intensities were corrected for absorption based on empirical ψ scans (S.D.P./ENRAF-NONIUS package). Lattice parameters were obtained by least-squares refinement of angular settings from 25 reflections. The refinements of the structures by least squares were based on F amplitudes with $w = 1/\sigma^2(F_o)$ by using block-diagonal method. All non-hydrogen atoms were refined with anisotropic thermal motion. The hydrogen atoms in calculated positions were

Table 1. Atomic positional parameters and B_{eq} for BBO_5O_5 ; $B_{\text{eq}} = 4/3 \sum_i \sum_j \beta_{ij} a_i a_j$

	x	y	z	Beq
O(1)	0.5745 (2)	0.1179 (1)	0.2199 (3)	4.4 (1)
C(2)	0.5702 (3)	0.0543 (1)	0.1719 (4)	3.4 (2)
O(3)	0.6295 (2)	0.0448 (1)	0.0488 (3)	4.0 (1)
C(4)	0.7531 (3)	0.0386 (1)	0.1100 (4)	3.5 (2)
C(5)	0.8175 (3)	0.0786 (1)	0.0421 (4)	3.2 (2)
C(6)	0.9410 (3)	0.0743 (1)	0.0961 (4)	3.2 (2)
C(7)	0.9963 (3)	0.0302 (1)	0.2206 (4)	2.7 (1)
C(8)	0.9298 (3)	-0.0117 (1)	0.2838 (4)	3.1 (2)
C(9)	0.8079 (3)	-0.0079 (1)	0.2268 (4)	3.3 (2)
O(10)	1.1167 (2)	0.0237 (1)	0.2904 (3)	3.3 (1)
C(11)	1.1898 (3)	0.0653 (1)	0.2297 (4)	3.6 (2)
C(12)	1.3172 (3)	0.0513 (1)	0.3333 (4)	4.5 (2)
O(13)	1.3442 (2)	0.0690 (1)	0.5104 (3)	4.1 (1)
C(14)	1.3906 (3)	0.1315 (1)	0.5444 (5)	4.6 (2)
C(15)	1.4081 (3)	0.1482 (2)	0.7288 (5)	4.7 (2)
O(16)	1.2974 (2)	0.1643 (1)	0.7480 (3)	3.8 (1)
C(17)	1.3089 (3)	0.1824 (2)	0.9198 (4)	5.0 (2)
C(18)	1.1921 (3)	0.1997 (1)	0.9361 (4)	4.5 (2)
O(19)	1.1575 (2)	0.2604 (1)	0.8644 (2)	3.3 (1)
C(20)	1.0668 (3)	0.2896 (1)	0.9199 (4)	3.1 (1)
C(21)	0.9456 (3)	0.2813 (1)	0.7908 (4)	2.9 (1)
O(22)	0.9138 (2)	0.2159 (1)	0.7943 (2)	3.4 (1)
C(23)	0.8255 (2)	0.1937 (1)	0.6511 (4)	3.0 (2)
C(24)	0.8245 (3)	0.1293 (1)	0.6255 (4)	3.0 (2)
C(25)	0.7427 (3)	0.1018 (1)	0.4838 (4)	2.8 (1)
C(26)	0.6610 (2)	0.1395 (1)	0.3678 (4)	2.9 (1)
C(27)	0.6595 (3)	0.2040 (1)	0.3935 (4)	3.2 (2)
C(28)	0.7417 (3)	0.2316 (1)	0.5360 (4)	3.7 (2)

Table 2. Atomic positional parameters and B_{eq} for $\text{Na}^+ \subset \text{BBO}_5\text{O}_5$; $B_{\text{eq}} = 4/3 \sum_i \sum_j \beta_{ij} a_i a_j$

	x	y	z	Beq
Na(30)	-0.1944 (4)	0.7394 (3)	0.3443 (2)	5.4 (2)
C1(31)	0.1791 (2)	0.7433 (2)	0.2790 (1)	5.6 (1)
O(32)	0.2942 (9)	0.8045 (7)	0.2947 (6)	11.1 (7)
O(33)	0.163 (1)	0.741 (1)	0.2083 (5)	13.0 (7)
O(34)	0.0457 (8)	0.7728 (7)	0.3078 (5)	9.7 (6)
O(35)	0.218 (1)	0.6588 (6)	0.3082 (6)	11.5 (7)
O(40)	-0.4382 (8)	0.6852 (6)	0.3500 (4)	6.9 (4)
O(1)	-0.4283 (8)	0.8930 (6)	0.0076 (4)	7.0 (4)
C(2)	-0.396 (1)	0.8128 (9)	-0.0300 (6)	6.8 (6)
O(3)	-0.4836 (8)	0.7369 (6)	-0.0068 (4)	7.2 (4)
C(4)	-0.433 (1)	0.6897 (7)	0.0497 (5)	5.3 (5)
C(5)	-0.512 (1)	0.6981 (7)	0.1122 (6)	5.1 (5)
C(6)	-0.460 (1)	0.6535 (7)	0.1680 (5)	4.9 (5)
C(7)	-0.327 (1)	0.6047 (6)	0.1663 (5)	5.3 (5)
C(8)	-0.253 (1)	0.5951 (7)	0.1036 (5)	5.4 (5)
C(9)	-0.307 (1)	0.6374 (7)	0.0457 (5)	5.9 (5)
O(10)	-0.2843 (7)	0.5661 (5)	0.2288 (4)	6.0 (4)
C(11)	-0.131 (1)	0.5371 (7)	0.2330 (6)	6.4 (6)
C(12)	-0.107 (1)	0.5030 (8)	0.3039 (7)	7.5 (7)
O(13)	-0.1403 (8)	0.5707 (5)	0.3551 (4)	6.4 (4)
C(14)	-0.073 (1)	0.5491 (8)	0.4186 (6)	8.1 (7)
C(15)	-0.144 (1)	0.607 (1)	0.4746 (6)	7.0 (6)
O(16)	-0.1299 (8)	0.7001 (5)	0.4605 (4)	6.6 (4)
C(17)	-0.193 (1)	0.759 (1)	0.5121 (5)	8.4 (8)
C(18)	-0.176 (1)	0.8539 (9)	0.4889 (6)	7.6 (7)
O(19)	-0.2552 (8)	0.8644 (5)	0.4253 (3)	6.6 (4)
C(20)	-0.252 (2)	0.9520 (8)	0.3970 (6)	7.4 (7)
C(21)	-0.337 (1)	0.9546 (7)	0.3306 (5)	6.8 (6)
O(22)	-0.2652 (7)	0.8925 (4)	0.2836 (3)	5.4 (3)
C(23)	-0.309 (1)	0.8974 (6)	0.2153 (5)	4.4 (4)
C(24)	-0.2141 (9)	0.8597 (6)	0.1678 (5)	4.3 (4)
C(25)	-0.247 (1)	0.8601 (7)	0.0990 (5)	4.8 (5)
C(26)	-0.383 (1)	0.8953 (7)	0.0762 (5)	5.3 (5)
C(27)	-0.479 (1)	0.9345 (7)	0.1238 (5)	4.9 (5)
C(28)	-0.443 (1)	0.9366 (7)	0.1932 (6)	5.6 (5)

refined isotropically. The drawing of the molecules was obtained by the SNOOPI program^[12]. Local programs were used both for refinement and Fourier synthesis (for atomic parameters see Tables 1, 2). — *Specific Data*: Free ligand 4: $\text{C}_{21}\text{H}_{26}\text{O}_7$; monoclinic; $P2_1/c$; $Z = 4$; $a = 1192.7(2)$, $b = 2120.9(1)$, $c = 820.8(1)$ pm; $\beta = 108.63(1)^\circ$; $V = 1967.5 \times 10^{-30} \text{ m}^3$. 3021 independent reflections were collected, of which 1904 were considered to be observed according to $I > 3\sigma(I)$. The structure was solved by direct methods using the MITHRIL package^[13]; $R = 0.057$ ($R_w = 0.035$; $s = 0.7$) with residual electronic densities less than $0.4 \text{ e}/\text{\AA}^3$. — Complex 4: $\text{NaClO}_4 \cdot \text{H}_2\text{O}$; orthorhombic; $P2_12_12_1$; $Z = 4$; $a = 897.3(1)$, $b = 1452.0(1)$, $c = 1927.3(1)$ pm; $V = 2502.6 \times 10^{-30} \text{ m}^3$. 1818 reflections were collected of which 1067 were considered to be observed according to $I > 3\sigma(I)$. The structure was solved by direct methods using the SHELX 86 program^[14]; $R = 0.060$ ($R_w = 0.062$; $s = 1.52$) with residual electronic densities less than $0.5 \text{ e}/\text{\AA}^3$.

[1] Part 1: H. Hopf, R. Utermöhlen, P. G. Jones, J.-P. Desvergne, H. Bouas-Laurent, *J. Org. Chem.* **1992**, *57*, 5509–5517.

[2] [2a] D. J. Cram, H. Steinberg, *J. Am. Chem. Soc.* **1951**, *73*, 5691. — [2b] P. M. Keehn, S. M. Rosenfeld (eds.), *The Cyclophanes*, Vol. I and II, Academic Press, New York, **1983**. — [2c] F. Vögtle, *Cyclophan-Chemie*, Teubner Studienbücher, Stuttgart, **1990**. — [2d] F. Vögtle, *Top. Curr. Chem.* **1983**, *113*, 1; **1983**, *115*, 2. — [2e] F. Diederich, *Cyclophanes*, The Royal Society of Chemistry, London, **1991**.

[3] [3a] J. F. Stoddart in *Frontiers in Supramolecular Organic Chemistry and Photochemistry*, (Eds.: H. J. Schneider, H. Dürr), VCH Verlagsgesellschaft, Weinheim, **1990**, pp. 251–263. — [3b] J. F. Stoddart, *Chem. Br.* **1991**, *27*, 714–718.

[4] [4a] P. Ruggli, *Justus Liebigs Ann. Chem.* **1912**, *392*, 92. — [4b] L. Rossa, F. Vögtle, *Top. Curr. Chem.* **1983**, *113*, 1. — [4c] B. Dietrich, P. Viout, J. M. Lehn, *Aspects de la Chimie des Composés Macrocycliques*, Inter Editions et Ed. du CNRS, **1991**, pp. 39–42.

[5] J. B. Birks, *Photophysics of Aromatic Molecules*, J. Wiley, London, **1970**.

- ^[6] H. Bouas-Laurent, R. Lapouyade, A. Castellan, A. Nourmode, E. Chandross, *Z. Phys. Chem. (Munich)* **1976**, *101*, 39–44.
- ^[7] J. Ferguson, *Chem. Rev.* **1986**, *86*, 957–982.
- ^[8] H. Bouas-Laurent, A. Castellan, M. Daney, J.-P. Desvergne, G. Guinand, P. Marsau, M.-H. Riffaud, *J. Am. Chem. Soc.* **1986**, *108*, 315–317.
- ^[9] J. B. Birks, *Photophysics of Aromatic Molecules*, J. Wiley, London, **1970**, p. 130.
- ^[10] I. B. Berlman, *Handbook of Fluorescence Spectra of Aromatic Molecules*, 2nd ed., Academic Press, New York, **1971**, p. 200.
- ^[11] Further details of the crystal structure investigation(s) are available on request from the Fachinformationszentrum Karlsruhe, Gesellschaft für wissenschaftlich-technische Information mbH, D-7514 Eggenstein-Leopoldshafen 2, on quoting the depository number CSD-57056, the names of the authors, and the journal citation.
- ^[12] K. Davies, private communication.
- ^[13] C. J. Gilmore, *J. Appl. Crystallogr.* **1984**, *17*, 42–46.
- ^[14] G. M. Sheldrick in *Crystallographic Computing 3*, (Eds.: G. M. Sheldrick, C. Krüger, R. Goddard), Oxford University Press, **1985**.

[417/92]